LOW-TEMPERATURE PHASE TRANSFORMATIONS PHENOMENA IN THE Al-21.5%Si ALLOY

ALEXANDER V. MAZUR, MICHAEL M. GASIK*

Helsinki University of Technology – TKK, P. O. Box 6200, FIN-02015 TKK, Finland

Received 19 September 2005, accepted 20 October 2005

The alloy Al-21.5%Si was studied with simultaneous thermal analysis, dilatometry, XRD, SEM and optical microscopy for analysis of its phase transformations in the solid state at the range 20–400 °C. Microstructure and phase composition were investigated on heat-treated and quenched samples and the phenomenon of silicon redistribution of α-Al solid solution was observed.

K e y w o r d s: aluminium alloys, silicon, phase transformations, heat treatment, thermal analysis

1. Introduction

In the binary (unalloyed) Al-Si alloys a large variety of microstructures and features are observed in both cast and heat-treated states. These microstructures are almost impossible to explain and to fit into simple eutectic phase stability diagram of the Al-Si system. Large volumetric fraction of α-Al solid solution, primary β-Si crystals and eutectic bi-crystallites make critical their influence on resulting structure and the properties of the castings. The understanding of the structural transformations, microstructure variations and associated properties is of a vital importance to improvement of the casting process and resulting properties level. In this work, the alloy Al-21.5wt.%Si was studied with simultaneous thermal analysis, dilatometry, XRD, SEM and optical microscopy for its microstructure transformations in the solid state at 20–400 °C. Microstructure and phase compositions were investigated on heat-treated and quenched samples and suggestions on the processes mechanisms are presented.

*corresponding author, e-mail: mgasik@pop.hut.fi

2. Experimental

The Al-21.5wt.%Si alloy with a total sum of technological impurities of 0.26 wt.% (0.22 % Fe, others (Cu, Ni, Mg, Mn, Ti, Pb, Zn, Cr, Zr) of < 0.005–0.01 % each) was melted and homogenised in alumina crucibles in a resistance furnace. The concentration of the impurities was much lower than their solubility limits in the α-phase [1]. After overheating to 1037 ℃, the melt was cooled down to 830 ℃ with rate of 10 K/min, soaked for 2 h and poured into a massive (8 kg) steel mould after surface dross removal. The temperature of the steel mould was 20 ℃ before casting, and it did not exceed 100 ℃ at a crystallisation of the sample. The cast specimen size was 16 mm diameter and 60–70 mm length, of the as cast density 2.45 g/cm^3. This procedure was supposed to simulate a common casting practice for this alloy [1, 2]. In this work, no special studies were made in regard to solidification kinetics, undercooling etc. features. It is clear that the casting structure is usually not uniform and certainly non-equilibrium. The emphasis of studies was on the transformations of the microstructures and properties of the alloy during heat treatment.

Simultaneous thermal analysis (STA) of the alloy (DSC, TG) was performed on the Netzsch STA449C "Jupiter" device (sample mass 150–170 mg, cut off the middle of the cast ingot). Empty alumina crucible was used as a reference. Dilatometry runs (DIL) with the same conditions were made on Netzsch DIL402C contact dilatometer (constant load of 0.3 N, specimen lengths 10–12 mm) in the range of 20–400 ℃ with the same scan rate of 10 K/min in pure argon. The methods of analysis and calibration were standard ones and they are described elsewhere [3] in more detail. Specimens were subjected to a heat treatment (up to 2 h soaking) at different selected temperatures to simulate STA and DIL experiments. After heat treatment the specimens were quenched from these temperatures in ice water.

Microstructure analysis was made using optical microscopy (Olympus PMG-3) and scanning electron microscopy (LEO 1450) with LINK system in the EDS mode. X-ray diffraction analysis was made using DRON UM-1 diffractometer with a high-temperature device UVD-2000 (accuracy $\pm$ 2 ℃, pure helium purge) with monochrome CuK$_\alpha$ radiation in the 2Θ-range of $10 \ldots 98°$. Silicon powder of semiconductor purity was used for an internal XRD standard. Experimental data were processed with dedicated software "Proteus 4.3", "PowderCell 2.4" and "CaRIne 3.1". Evaluation of microstructure features was done with "SigmaScan Pro 5.1" and "OOF" packages.

3. Results

The results of thermal analysis of a cast sample are shown on Fig. 1. DSC curve exhibits a clear exothermal process in the range of $220 \ldots 310$ ℃, having the maximum (peak) of the process near 260 ℃. The integral heat release during

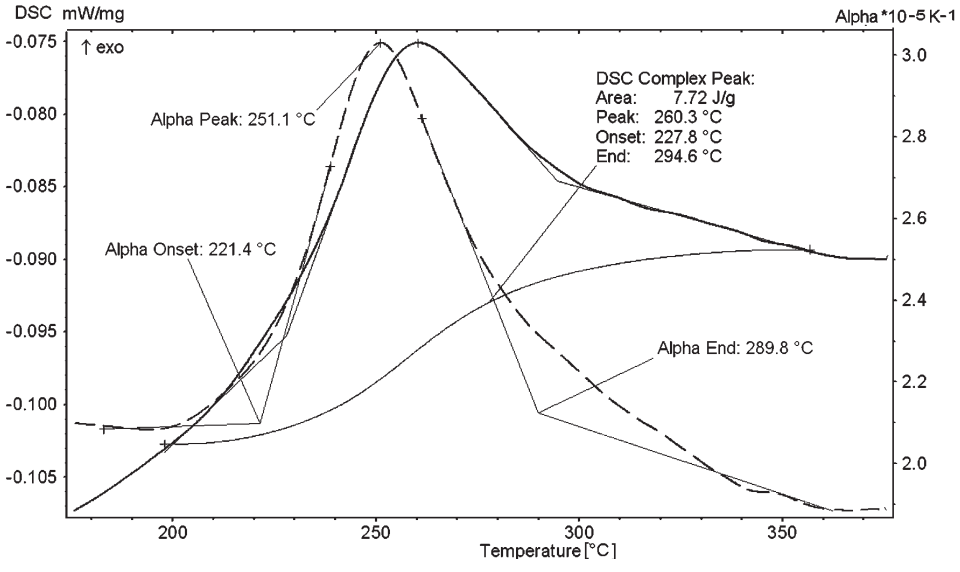

Fig. 1. Thermal analysis (DSC and dilatometry) of the Al-21.5%Si alloy. Underlined onset, peak and end values are referred to CTE, complex peak analysis – to DSC curve.

Table 1. Lattice parameters of α-Al solid solution [nm] and thermal expansivity Δ calculated of XRD data. Lattice expansivity of pure aluminum Δa_{Al} is calculated from data [2] by Eq. (1)

T [°C]	$a_{\alpha\text{-Al}}$ [nm]	Δa_{α} [%]	Δa_{Al} [%]	Δ [%]
20	0.405071	0	0	
230	0.407023	0.482	0.535	−9.935
305	0.407792	0.671	0.740	−9.248
350	0.408263	0.788	0.866	−9.052
400	0.409433	0.919	1.010	−9.010

heating of the samples was about 7700 J/kg in this range, determined by the peak area. No other significant reproducible thermal processes were found among other temperatures up to 400 °C. Dilatometry (Fig. 1) shows an abnormal (more than 2 times) increase of the thermal expansion coefficient (CTE) in the same range of temperatures as for mentioned exothermic effect. The correlation of the experimentally observed phenomena might be treated as excellent despite they have been received with different methods.

XRD was applied for evaluation lattice parameters of α-Al phase, Table 1, to evaluate proper correlation with CTE results. Because the lattice parameter is

affected not only by temperature, but also by (a priori unknown) dissolved silicon concentration and possible residual stresses, it was related to the lattice parameter changes of pure aluminium by equation

$$\Delta = \frac{\Delta a_\alpha - \Delta a_{\mathrm{Al}}}{\Delta a_{\mathrm{Al}}}; \quad \Delta a_i = \frac{a_i(T) - a_i(0)}{a_i(0)}, \tag{1}$$

with Δa being lattice parameter change of the i-phase (pure Al or the α-solid solution) at the temperature T in relation to the room temperature $a_i(0)$, Δ – the relative thermal expansivity of α-solid solution in respect to pure aluminium. In this way the possible effect of other factors on lattice expansion is supposed to be minimised.

As seen from Table 1, this Δ parameter deviates from a linear behaviour in the range of 230 . . . 305 ℃. This increased expansivity from XRD data formally coincides with the temperature range of maximal CTE values (Fig. 1). Pure aluminium and silicon do not exhibit significant CTE deviations nor lattice parameter variations in this temperature range [4]. In this respect, it might be possible the effects observed by DSC and DIL are associated with some process related to α-phase and its transformations.

For determination of the phenomena and possible mechanism of exothermal effect and CTE peak, as-cast specimens were heated and quenched from 250 ℃ and from 400 ℃. The temperatures selection is self-evident from Fig. 1. The typical microstructures of these specimens are shown on Fig. 2 together with the original cast structure. The following structural constituents (SC1, SC2, SC3) were found out and identified as primary "excess" crystals of β-Si (K), distinct grains of a solid solution (SC1, SC2) and structures of the cooperative growth (E1, E2, E3), Table 2. The latter ones have different composition and microstructure features, depending on the heat-treatment temperature. K-crystals (β-phase) of cubic or hexagonal habit have practically remained unaffected by heat treatment procedure and are not especially considered here.

In the α-solid solution of the cast structure (SC1), silicon concentration is varied from 1.55 up to 2.35 at.% (in the centre of the grain) as measured by EDS (cobalt standard calibration). Silicon concentration in the centre of the grain of the cast specimen was by $\sim 1/3$ higher than on the edges. In the specimens quenched from 250 ℃ silicon distribution in the Al-based solid solution SC2 (later shown as α'-Al phase) has changed to alternating one with "high-Si" zones (up to 2.1 at.% Si) and "low-Si" zones (1.6 . . . 1.7 at.% Si). The spacing between these zones was of 3 . . . 5 μm, Fig. 3. It is necessary to notice that the Si-concentration has exceeded the greatest possible value in the α-phase according to the stable phase diagram [1]. The total silicon concentration in the α-phase did not yet significantly change and thus major expansivity (1) variations might indeed be associated with temperature and residual stresses effects.

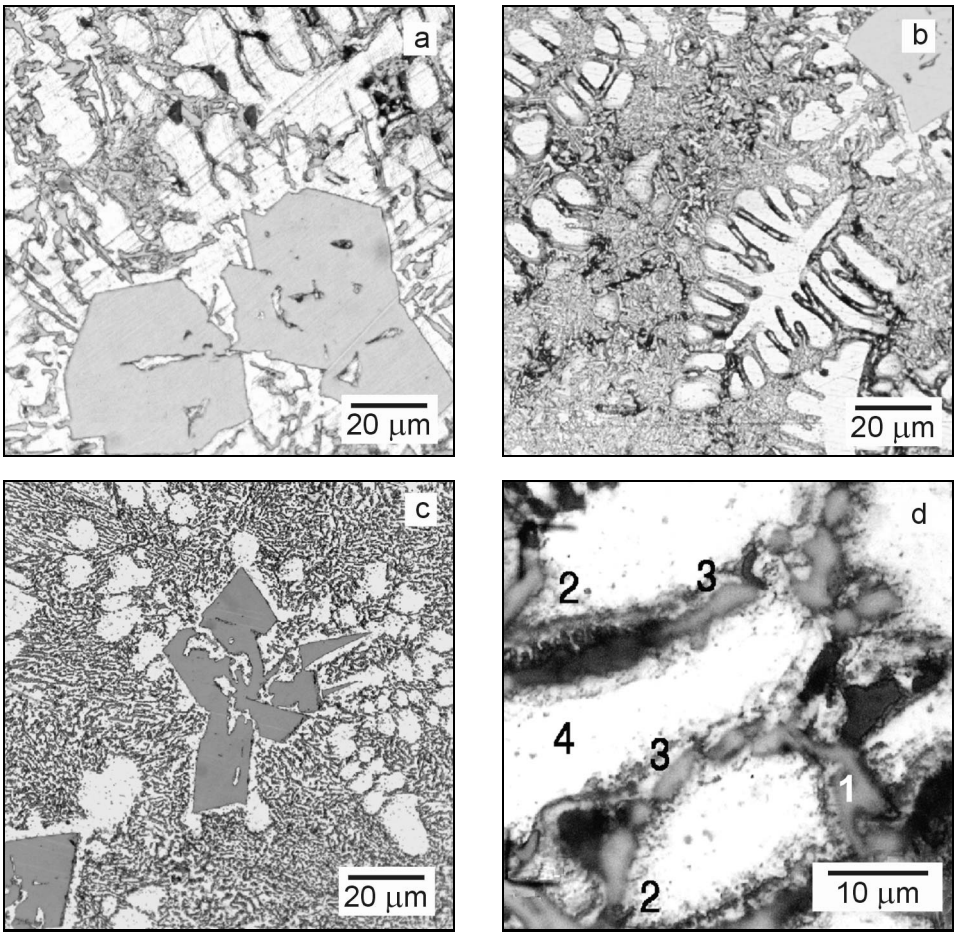

Fig. 2. Microstructures of the Al-21.5%Si alloy as cast (a), heat-treated at 250 ℃ (b, d – at higher magnification) and 400 ℃ (c). Photos (a–c) are of the same magnification. The "painted edges" can be seen in Fig. 2d. At the Fig. 2d the structural constituents are shown as: 1 – β-Si_{eut}, 2 – "painted edges", 3 – β-Si_{perit}, 4 – α'-Al.

The amount of heat released in this range (220 . . . 310 ℃) cannot be explained solely by changes of α-Al solid solution composition because there were no significant visible precipitations of silicon (except for the edges), Fig. 2. Thus heat of possible α-phase decomposition cannot solely cover the whole amount of energy released during heating, observed in experiments.

The third structural constituent (SC3, quenched from 400 ℃) looks eventually similar to SC2 with a light optical microscopy. However, high-magnification

Table 2. Microstructure features observed in cast and heat-treated Al-Si alloy (primary excess silicon crystals (K) are not shown). Microhardness is marked by (μ)

Type of the microstructure constituents	Hardness [GPa]	Specimens state, phase composition
E1 – the conglomerated, irregular eutectics. The cross-sections size of needle crystals 2 . . . 5 μm.	1.71	As-cast $(\alpha + \beta)$
E2 – similar to E1 structure of cooperative growth (solid solution and two phases with lighter- and darker-etched needle-like round-edged crystals). The cross-sections size of needle crystals 0.3 . . . 1.0 μm.	1.76	Heat-treated 250 °C $\alpha + (\alpha' + \mathrm{Si})$
E3 – bi-crystallite of cubic-like cooperative growth, with irregular plate-like dendrites. The cross-sections size 1 . . . 2 μm.	5.33	Heat-treated 400 °C $(\mathrm{Al} + \mathrm{Si})_{\mathrm{perit}} + \beta$
SC1 – rounded equiaxed lighter-etched dendrites with only the first order branches of the cross-sections size 20 . . . 60 μm.	0.22 (μ)	As-cast α
SC2 – round-branched lighter-etched dendrites creating a "fern-leave" pattern. The axes ratio of the dendrites of 3 . . . 20 and more with mutually orthogonal branches. Cross-sections of the branches 1.5 . . . 6.0 μm.	1.40 (μ)	Heat-treated 250 °C α'
SC3 – the two-phases structural component generated from SC2. It consists of Al-matrix and thin (0.3 . . . 0.5 μm) silicon platelets.	1.68 (μ)	Heat-treated 400 °C $(\mathrm{Al} + \mathrm{Si})_{\mathrm{perit}}$

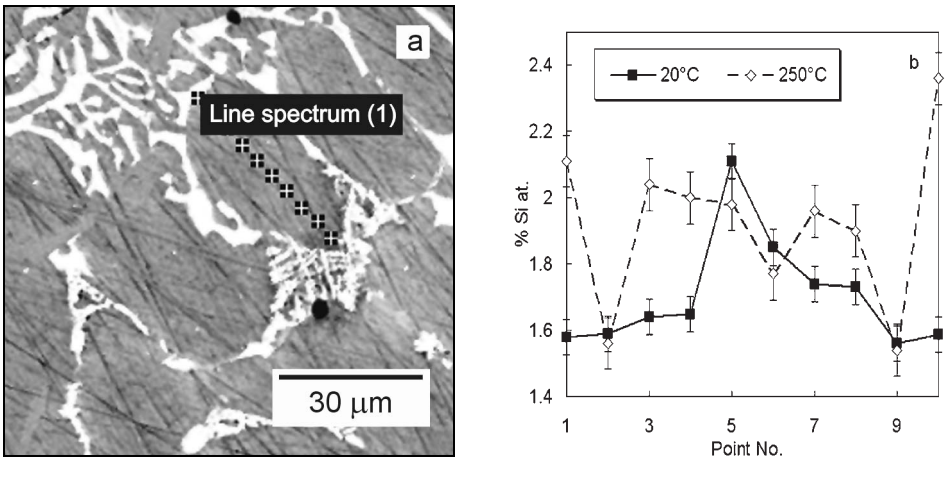

Fig. 3. SEM picture of the alloy and analysed silicon concentration across the solid solution grain (as cast and heat treated at 250 °C).

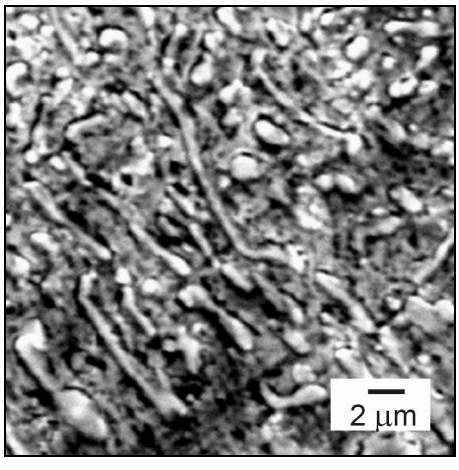

Fig. 4. Fine silicon precipitates formed from the solid solution at 400 °C.

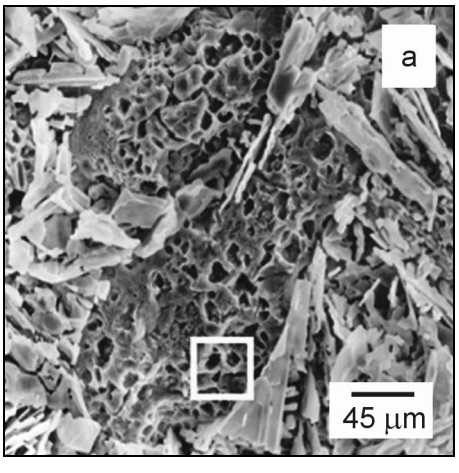

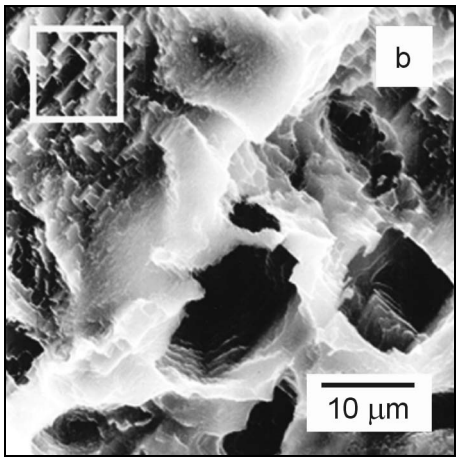

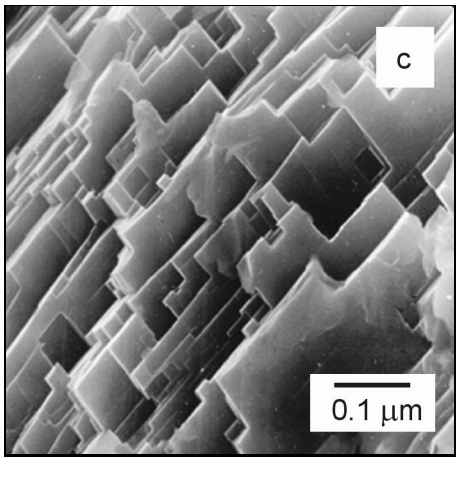

Fig. 5. Silicon appearance from the solid solution (aluminium was deeply etched). Boxes indicate approximate places of pictures taken of the right (box size of Fig. 5a is $\sim$ 45 μm; 5b $\sim$ 10 μm).

SEM examination reveals SC3 in this case has decomposed on practically pure Al (< 0.1 % Si) zones and small (thickness of ~ 100 nm), parallel-oriented plate-like silicon inclusions, Fig. 4. Thus SC3 is not a true solid solution, but a composition of aluminium and very fine silicon precipitates. They become visible in SEM after deep etching off aluminium, Fig. 5. On the contrary of effects at 250 ℃, there were no significant thermal either expansion effects despite clear changes of α'-phase and formation of aluminium and silicon precipitates. This supports previous hypothesis about exothermal effect at 250 ℃ – an additional energy release origin (besides silicon precipitation) should be present in cast structure vs. heat-treated one.

XRD examination did not found any unknown reflections from phases besides α-Al and β-Si. There were also no reflections from intermetallics or oxides, which may be formed by impurities. Thus possible contribution of any additional or unknown phases in these transformation processes is very unlikely.

4. Discussion

The changes in microstructures of the alloy after heat treatment might be summarised in the following. After 250 ℃, the morphology of SC1 solid solution has changed to SC2 (Table 2) affecting structural type of the co-growth crystallites. Eutectic-like structure E2 has formed instead of E1. Both SC2 and E2 have areas (edges) with looks "painted", Fig. 2d. Such areas are normally signs of the parent phase replacement by the mechanism of peritectoid reaction [3, 5, 6]. Formation of "painted" edges in this case is based on different solubility of the component in the metastable phase than in a stable phase in these particular conditions. Based on the structural features observed, such peritectoid-like transformation might be formally expressed by the reaction $\alpha \rightarrow (\alpha' + \beta\text{-Si})_{\text{perit}}$. The process of disintegration α-Al (SC1) by peritectoid mechanism is carried out with simultaneous increase of the cumulative contents Si in SC2 as contrasted to SC1. The formation of the light-etched peritectoid genesis β-Si plates on the boundaries of α'-Al grains becomes possible due to diffusion of atoms Si from eutectic laminas of β-phase which are disintegrated.

It is known, that low-temperature peritectoid reaction proceeds, as a rule, under non-equilibrium conditions [7] resulting in peritectoid structure with a feature of order of 20 nm (with a driving force for nucleation of the product phase of the order of 100 J/mol, a surface energy of 1 J/m^2, and an atomic volume of 10 cm^3/mol). This is lower than the detection of optical and even conventional scanning electron microscopy. This is reported to eliminate the dependence of the growth kinetics from the component concentration in the parental phase.

In the case of studied Al-Si alloy, the exothermal process in the range of 220 . . . 310 ℃ was accompanied by a significant increase of CTE (Fig. 1). Figure 3 shows the different silicon concentration distribution in the α-Al and α'-Al solid

solutions. The average silicon content has increased from 1.7 at.% Si in SC1 to 2.0 at.% Si in SC2. However, by present investigation it was not possible to check microscopically, whether SC2 retains a solid solution or forms extremely fine precipitates (either coherent or not). Since SC2 exists only accompanied by the phase with "painted edges", it indeed may remain a true (yet a non-equilibrium) solid solution. This indicates that the transformation process might thus not be finished in samples quenched from 250 ℃. A significant variation in silicon concentration in the solid solution without visual appearance of silicon as a free phase constituent suggests this to be an intermediate state. After heat treatment at 400 ℃, the process results in the formation of stacks of silicon plates (Figs. 4, 5), which are visible at normal SEM resolution levels. Although TEM is more proper technique for analysis of that phenomenon, it was not the main objective of the present work.

These microstructure features allow suggesting a hypothesis that "peritectoid" silicon plates did appear due to short-range up-hill collective diffusion of silicon atoms (Fig. 6). Normally, silicon is expected to form a solid solution in Al by a substitution type, which supposes a levelling diffusion to take place [8]. However, energy accumulation and release due to both local (coherent lattice) misfit and meso/macroscopic (caused by phases' CTE) strains misfit cause changes in the total energy of the system at different levels [7]. For majority of thermodynamic simulations and phase diagrams calculations the system free Gibbs energy is composed of the sum of chemical potentials and excess free energy, defined to be uniform across the system [2, 8]. A non-homogeneous material at microlevel would have local variations of free energy, caused by elastic stresses (local pressure), surface energy, local gradients in composition, etc. [9–12]. Generally, free energy change dE for the local conditions of a space-limited crystal might be approximated by

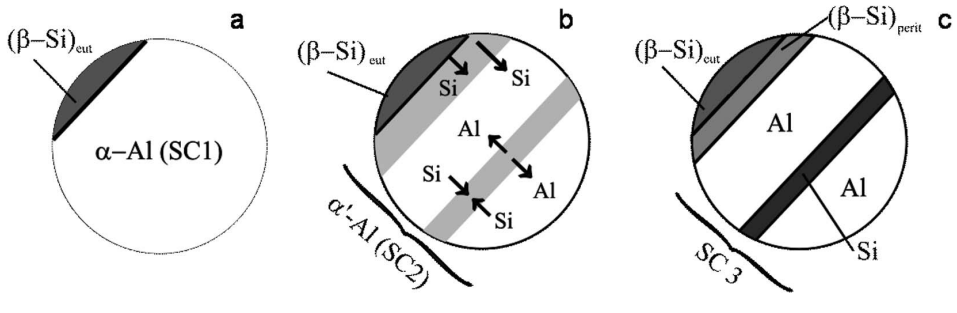

Fig. 6. A scheme of the transformation of α-phase (SC1, Table 2): a – as cast, b – process at 250 ℃, c – process result after heat treatment at 400 ℃. Diffusion directions are indicated by arrows.

equation

$$\mathrm{d}E = \mathrm{d}\sum_i \left.\frac{\partial E_i}{\partial n_i}\right|_{n_j,P,T,V} \cdot n_i + \mathrm{d}(PV) + \mathrm{d}(TS) + \mathrm{d}(\gamma A) + \mathrm{d}(\sigma\varepsilon) + \mathrm{d}\left(\frac{1}{2}\chi\left(\nabla C\right)^2\right) + \mathrm{d}W_{\mathrm{ext}}, \tag{2}$$

where: $(\partial E_i/\partial n_i)$ – partial free energy of the component i, n_i, n_j – numbers of moles, P – "external" pressure, V – volume, T – absolute temperature, S – entropy, γ – surface energy of interfaces between the phases, A – interfaces surface area, σ – local elastic stresses tensor, ε – local elastic strains tensor, C – local concentration of the component, χ – a coupling constant [13], and W_{ext} – energy of external and other forces, which may include for instance the energy of the dislocation systems. The method of local equilibrium is widely used in analysing e.g. diffusion problems, with the approach of phase field, gradient thermodynamics and other methods [9–13]. The process in the system may proceed at constant P, T, μ, n, not only due to volume or entropy changes, but also by changing gradients of concentration, interfaces state and surface or accumulated elastic energy. If the surface energy term is large, the system would likely to move towards smaller surface area (coalescence, grain growth). If the elastic energy is large, the system may change its state so smaller sizes of phase constituents would be more beneficial.

Cahn and Hilliard have shown that elastic strain gradients can cause an additional diffusion flux of a component even if there are no gradients of concentration, chemical potential, pressure or temperature [12]. It is also known that elastic energy might stabilise a solid solution, which would be unstable under classical Gibbs energy analysis normally applied for phase diagram calculations [11–18]. Elastic energy contribution might even create special singular points of the two-phase areas (Williams points), impossible from the conventional analysis point of view [13–15].

In this study, the concept of mesoscopic elastic energy change, responsible for a phase transformation [11, 13, 14], is applied to specific microstructures and thermal effects found in the Al-Si alloy. For both microscopic level (lattice) and mesoscopic level (visually observed microstructure) there exists a misfit due to different CTE of α- and β-phases. Because at 250 °C the silicon content in the α'-Al phase seems to remain similar to cast structure, microscopic (lattice) misfit variations (whether coherent or not) are of a minor importance for the present case. Supposing that the eutectic temperature (577 °C) corresponds to the stress-free state, subsequent cooling will generate local stresses (nearly tensile in α-Al and compressive in β-Si) when quenched. Heat treatment should release these stresses (in fact, stored elastic energy), but if the conditions are favourable, the phase transformation might also occur [11, 13–17]. Williams [14] has presented the practical application of this method to phase diagrams analysis, but he has pointed out the importance of the knowledge of the stresses and energy distribution in real microstructures. At that

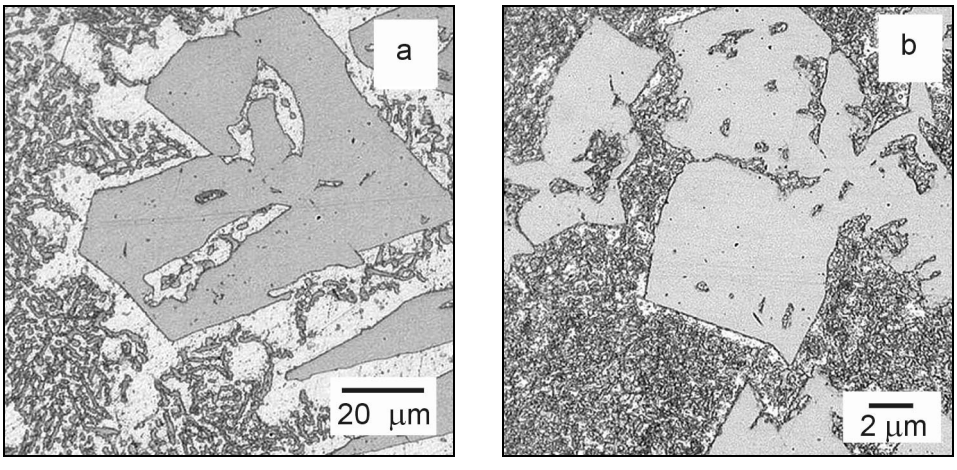

Fig. 7. Microstructures of cast (a) and heat-treated (b) at 250 °C alloys taken for analysis of the elastic energy distribution. Magnification is the same as for Fig. 2 (a–c).

Table 3. Assessed elastic constants [GPa] of aluminium- and silicon-rich phases [2]

Elastic constants	α-Al	β-Si
C_{11}	$117.4 - 0.044 \cdot T$	$163.8 - 0.0128 \cdot T$
C_{12}	$62.407 - 0.0073 \cdot T$	$59.2 - 0.0048 \cdot T$
C_{44}	$31.259 - 0.0088 \cdot T$	$81.7 - 0.0059 \cdot T$
Average anisotropy factor $= 2C_{44}/(C_{11}–C_{12})$	1.545	1.566

time, however, no computer algorithms were available to analyse the differences in microstructures with a high reliability.

Figure 7 demonstrates two microstructures with the same magnification taken as-cast and after heat treatment at 250 °C. The volume fractions of α- and β--phases here are almost the same. For these phases, elastic constants of aluminium and silicon were used as shown in Table 3. The microstructures of Fig. 7 have been converted into a binary format and then to the finite elements mesh using a standard adaptive routine with relaxation. The boundary conditions were set to reflect absence of traction forces and external loads, leaving only thermally induced loads for pure elastic regime.

Mesoscopic stresses, strains and finally elastic energy density were obtained for these microstructures (Fig. 8). To make a quantitative comparison, a normalised histogram of the elastic energy distribution was assessed based on these numerical data, Fig. 9. These figures clearly show that heat treatment at 250 °C results in

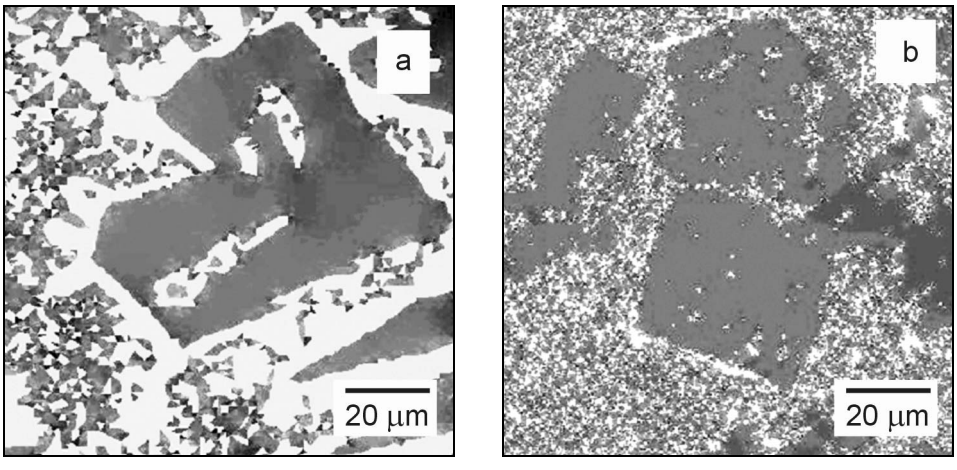

Fig. 8. Calculated elastic energy density for cast (a) and heat-treated at 250 °C (b) alloys. Light areas correspond to higher stresses and high elastic energy densities.

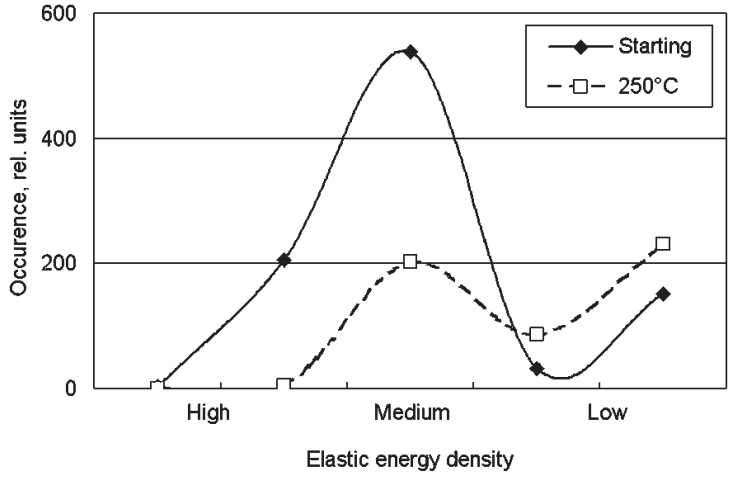

Fig. 9. Histogram of elastic energy density distribution (arbitrary units).

a significant decrease of the areas with the highest energy density (mainly of α--phase). It corresponds to the deductions [7] that the magnitude of the internal stresses in such structures can reach order of hundreds of MPa. Since the CTE of α-phase is almost six times higher than of β-phase despite lower elastic modulus, in

as-cast state α-phase would have substantial tensile strains. These would also affect the silicon solubility in the α-Al. Heating at 250 ℃ promotes such microstructure changes leading to a decreasing of elastic energy to 5–6 J/cm^3 (proportional to the area under the curve of the histogram) in comparison of $\sim$ 9 J/cm^3 for a cast structure. This result is in a remarkable agreement of the DSC data (Fig. 1), where $\sim$ 3 J/cm^3 ($\sim$ 7.7 J/g of alloy) energy release was recorded as heat. It is necessary to note that more calculations are needed to estimate energy density changes in the realistic 3-D case with higher accuracy because microstructures contain a lot of features of different scale, which affects suitable meshing procedure and may lead to loss of particular contributions.

During the heat treatment, retained SC2 grains "collect" silicon by diffusion (Fig. 3). These processes are believed to decrease the stressed state of the specimen both in macro- and meso-levels. Here phase size refining is taking place simultaneously with a formation and further annihilation of the structural defects that affects the total energy of the system [19].

Similar process was earlier observed in superalloys known as rafting with formation, growth and severe shape change of the 20–200 nm precipitates as a result of combined effect of diffusion and elastic energy changes [4, 13–19]. In the case of Al-Si cast alloy it is possible to conclude that SC2 (Table 2) "oversaturated" solid solution decomposes to aluminium-rich matrix and plate-like silicon (at 220 . . . 310 ℃) which then turns into a coupled growing bi-crystallite at 400 ℃ (Figs. 4, 5):

$$\alpha \xrightarrow{\tau,T} \alpha' + \beta \xrightarrow{\tau} (\mathrm{Al} + \mathrm{Si})_{\mathrm{perit}} + \beta. \tag{3}$$

It is important to distinguish the differences between the "ageing" effect (decomposition of oversaturated solid solution with temperature and time) and structural, morphological transformation (in this case by formation of periodically ordered skeletal Si-dendrite in α'-phase with simultaneous transformation to pure Al, Figs. 3–6). In the latter case the concentration of silicon in α-Al and α'-Al phases varies only a little and it is not the main feature of the process. In the case studied there are morphological changes of microstructures, which do not have character of the known ageing effect, even if it appears during the similar heat treatment procedure. There is also a possibility that surface energy may contribute significantly to the total free energy of the system (2). This was not explicitly considered in this work, but should be taken into account for a full analysis of such systems [17, 18].

5. Conclusions

1. The α-solid solution of a hypereutectic Al-Si alloy was found to transform in a temperature range of 220 . . . 310 ℃ into isomorphous α'-Al phase. This phase has different microstructure features and lattice parameters (for example, other morphology of the crystallites of cooperative growth).

The α-Al in the structure of the cast sample is likely to be under stretching (tensile) stresses. The specific elastic energy of an alloy is roughly estimated to be reduced by $\sim$ 30 % at its heating up to 250 ℃ owing to structural changes, as determined by a numerical calculation. These structural transformations and energy changes are characterised by an exothermal process, releasing $\sim$ 7700 J/kg of alloy.

2. The hypereutectic Al-Si alloy was demonstrated to have a sequence of the phase and microstructure transformations. They do not have character of the known ageing effect (precipitation of silicon from oversaturated solid solution), even if it appears during the similar heat treatment procedure. The concentration of silicon in α-Al and α'-Al phases was found to vary only a little with temperature. The α'-Al phase transforms into the bi-crystallite of cooperative growth at heating (310 . . . 400 ℃). This "rafting-like" bi-crystallite consists of almost pure aluminium and distinct silicon plates ($\sim$ 100 nm) stacks with an atomic-smooth surface. An additional work is necessary to study further possible transformations of the latter structure at higher temperatures, including a possible contribution of the surface energy to the total free energy of the system.

Acknowledgements

Financial support of the Academy of Finland (grants 75199, 79206, 210154) is gratefully acknowledged. Special thanks for M. Sc. M. Friman for the assistance in thermal analysis. Authors also thank Dr. E. Kaisersberger (Netzsch Gerätebau GmbH, Germany) for independent validation of DIL analysis of the alloy and to Prof. V. I. Mazur for scientific discussions.

REFERENCES

[1] MONDOLFO, L. F.: Aluminium Alloys: Structure and Properties. London, Butterworths 1976.
[2] Aluminum Handbook. Eds.: Totten, G. E., Mackenzie, D. S. New York, Basel, Marcel Dekker 2003.
[3] MAZUR, A. V.—GASIK, M. M.—MAZUR, V. I.: Z. Metallkd., *95*, 2004, p. 377.
[4] ROBERTS, R. B.: J. Phys. D: Appl. Phys., *14*, 1981, p. 163.
[5] SHIBATA, H.—ARAI, Y.—EMI, T.: Metall. Mater. Trans., *31B*, 2000, p. 981.
[6] RHINES, F. N.: Phase Diagrams in Metallurgy. New York, McGraw-Hill Books 1956.
[7] KLINGER, L.—BRECHET, Y.—PURDY, G.: Acta Mater., *46*, 1998, p. 2617.
[8] KUBASCHEWSKI, O.—ALCOCK, C. B.: Metallurgical Thermochemistry. 5th ed. Oxford, Pergamon Press 1979.
[9] CAHN, J. W.: Acta Metall., *25*, 1977, p. 1021.
[10] LEE, J. K.: Mater. Trans. JIM, *39*, 1998, p. 114.
[11] CAHN, J. W.—LARCHE, F.: Acta Metall., *32*, 1984, p. 1915.
[12] CAHN, J. W.—HILLIARD, J.: J. Chem. Phys., *28*, 1958, p. 258.
[13] FRATZL, P.—PENROSE, O.—LEBOWITZ, J. L.: J. Stat. Phys., *95*, 1999, p. 1429.
[14] WILLIAMS, R. O.: CALPHAD, *8*, 1984, p. 1.
[15] CAHN, J. W.—LARCHE, F.: Acta Metall., *21*, 1973, p. 1051.

[16] LARCHE, F.—CAHN, J. W.: Acta Metall., *26*, 1978, p. 1579.
[17] KHACHATURYAN, A. G.—SEMENOVSKAYA, S. V.—MORRIS, J. W.: Acta Metall., *36*, 1988, p. 1563.
[18] MCCORMACK, M.—KHACHATURYAN, A. G.—MORRIS, J. W.: Acta Metall. Mater., *40*, 1992, p. 325.
[19] GLATZEL, U.—FELLER-KNIEPMEIER, C.: Scripta Metall., *23*, 1989, p. 1834.